

# Chapter 7

## A Non-geostrophic Wet Q-vector Analysis of Continuous Heavyrain in Hunan



Haichao Cai, Jinjie Cai, Zhonghai Yin, Hongwu Liu, and Lu Wang

**Abstract** Using NCEP  $1^\circ \times 1^\circ$  reanalysis data, Conventional meteorological observation data and surface intensive observation data, the non-geostrophic Q vector theory, diagnostic analysis is performed in a continuous rainstorm process in Hunan from 2012 June 25 to 28. The results show that: the change of non-geostrophic Q-vector convergence zone is a good indication of the heavy precipitation area, stable and less strong Q-vector convergence center for persistent heavy rainfall occurred; Rainstorm peak, with a plurality of Q-vector divergence near the middle troposphere 400 hPa “positive–negative” center appear alternately, the heavy rainfall region is corresponding with the strong Q-vector divergence over the negative region, rainstorm process later, the Q-vector divergence “positive–negative” alternate center weaken and disappear, the rainfall is not only related with the non-geostrophic ascending motion, the non-geostrophic sinking motion role is very important, and the non-geostrophic rising region often heavy rain area and has a good corresponding relationship; The development of the torrential rain accompanied by secondary circulation, rainfall peak periods, respectively along the longitudinal and latitudinal is a “positive–negative” center are arranged alternately, and heavy rain area is located in the south of the West and often negative area negative area value secondary circulation interchange near the ascending branch.

**Keywords** Rainstorm · Non-geostrophic Q-vector · Secondary circulation

---

H. Cai  
Loudi Meteorological Bureau, Hunan Loudi 417000, China

J. Cai · Z. Yin (✉) · H. Liu · L. Wang  
Hunan Meteorological Observatory, Changsha 410000, China  
e-mail: [369543471@qq.com](mailto:369543471@qq.com)

H. Cai · J. Cai · Z. Yin · H. Liu · L. Wang  
Hunan Key Laboratory of Meteorological Disaster Prevention and Reduction, Changsha 410007, China

## 7.1 Introduction

Hunan Province is located on the south bank of the middle reaches of the Yangtze River, north of the Nanling Mountains. It is located between  $24^{\circ}38' \sim 30^{\circ}08' \text{ N}$  and  $108^{\circ}47' \sim 114^{\circ}15' \text{ E}$ . It belongs to the subtropical humid monsoon climate zone. Rainstorms are frequent, and persistent rainstorms often lead to floods, causing great harm to people's lives and property. Since 1978, Hoskins et al. (1978) proposed the concept of Q vector and derived the quasi-geostrophic  $\omega$  equation with its divergence as the only forcing term, which intuitively shows the strength of the forcing mechanism of  $\omega$ . Since the late 1980s, the quasi-geostrophic Q vector has been gradually applied to China's meteorological operations (Yang and Cao 1995; Yi et al. 1999; Shi et al. 2008; Song et al. 2009; Gao et al. 2018, 2019; Li and Li 2017; Ran et al. 2019). Subsequent studies have found that (Zhang 1999; Liu 2006; Li et al. 2002), the quasi-geostrophic Q vector is the result of assuming that the atmosphere is derived under adiabatic and quasi-geostrophic conditions, but it is not adiabatic for the actual atmosphere, especially in the rainstorm process. There is a large amount of condensation latent heat release, and the assumption of adiabatic conditions is very impractical. At the same time, due to the limitation of quasi-geostrophic approximation, it is not suitable for application in low latitudes, especially for the study of sub-synoptic scale motion. In 1998, Zhang (Zhang 1998) considered the effect of atmospheric condensation latent heat, put forward the concept of wet Q vector, and derived the expression of non-geostrophic wet Q vector and the non-geostrophic  $\omega$  equation with the divergence of wet Q vector as the only forcing term from the non-adiabatic original equations, which can more truly reflect the situation of the actual atmosphere corresponding to the generation and development of rainstorm in different latitudes. In recent years, more and more meteorological scholars have begun to study the persistent heavy rain, and have achieved certain results, but the study of persistent heavy rain in Hunan using Q vector theory is still rare. In this paper, using NCEP  $1^{\circ} \times 1^{\circ}$  reanalysis data and conventional meteorological observation data, the Q-vector diagnostic analysis was carried out on a persistent rainstorm weather process in Hunan from June 25 to 28, 2012. The variation characteristics of the corresponding non-geostrophic wet Q-vector during the rainstorm process and the manifestation of the sub-synoptic scale system were discussed, which provided some useful reference for the future persistent rainstorm forecast.

## 7.2 Non-geostrophic Wet Q Vector Expression

According to Reference (Chen et al. 2009), the non-geostrophic wet Q vector is defined as  $Q^* = (Q_x^*, Q_y^*)$ , and the expression is:

$$Q_{x^*} = \frac{1}{2} \left[ f \left( \frac{\partial v}{\partial p} \frac{\partial u}{\partial x} - \frac{\partial u}{\partial p} \frac{\partial v}{\partial x} \right) - h \frac{\partial V}{\partial x} \nabla \theta - \frac{\partial}{\partial x} \left( \frac{LR\omega}{C_p p} \cdot \frac{\partial q_s}{\partial p} \right) \right] \quad (7.1)$$

$$Q_{y^*} = \frac{1}{2} \left[ f \left( \frac{\partial v}{\partial p} \frac{\partial u}{\partial y} - \frac{\partial u}{\partial p} \frac{\partial v}{\partial y} \right) - h \frac{\partial V}{\partial y} \nabla \theta - \frac{\partial}{\partial y} \left( \frac{LR\omega}{C_p p} \cdot \frac{\partial q_s}{\partial p} \right) \right] \quad (7.2)$$

$Q_{x^*}$  and  $Q_{y^*}$  are the wet Q vector components in the x and y directions, respectively, where,

$$h = \frac{R}{p} \left( \frac{p}{1000} \right)^{R/C_p} \quad (7.3)$$

Other symbols are commonly used physical symbols. The formula of non-geostrophic wet Q vector shows that  $Q^*$  depends on the difference effect of horizontal shear and vertical shear of wind, the product of horizontal gradient of wind and horizontal gradient of temperature and non-adiabatic effect. The non-geostrophic  $\omega$  equation with the non-geostrophic wet Q vector divergence as the forcing term is:

$$\nabla^2(\sigma\omega) + f^2 \frac{\partial^2 \omega}{\partial p^2} = -2\nabla \cdot Q^* \quad (7.4)$$

$\nabla \cdot Q^*$  is the divergence of the non-geostrophic wet Q vector, assuming that the vertical motion of the atmosphere is a form of fluctuation,  $\omega \propto \nabla \cdot Q^*$ , when  $\nabla \cdot Q^* < 0$ ,  $\omega < 0$ , ascending motion; when  $\nabla \cdot Q^* > 0$ ,  $\omega > 0$ , sinking motion. In fact, it is the forcing mechanism of ascending motion that must excite the secondary circulation. The relationship between the non-geostrophic Q vector and the secondary circulation is:

$$Q_{x^*} = \frac{1}{2} \left( f^2 \frac{\partial u_a}{\partial p} - \sigma \frac{\partial \omega}{\partial x} \right) \quad (7.5)$$

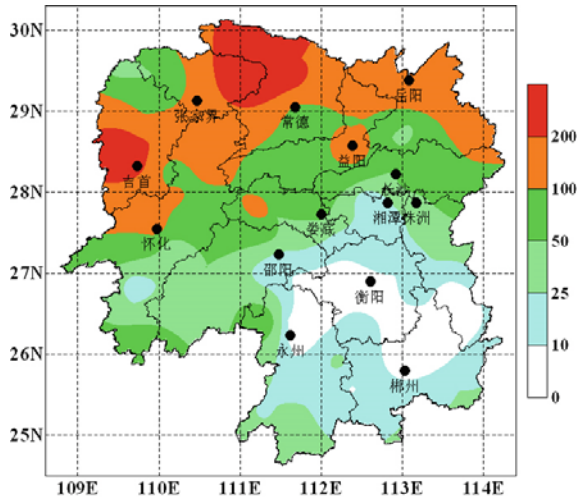
$$Q_{y^*} = \frac{1}{2} \left( f^2 \frac{\partial u_a}{\partial p} - \sigma \frac{\partial \omega}{\partial y} \right) \quad (7.6)$$

It can be seen that the zonal and meridional vertical circulation is determined by the zonal and meridional components of the non-geostrophic wet Q vector, respectively.  $Q_{x^*}$  and  $Q_{y^*}$  always point to the updraft area and back to the downdraft area.

### 7.3 Process Overview and Large Scale Circulation Analysis

From 08:00 on June 25 to 08:00 on June 28, 2012 (Beijing time, the same below), a continuous rainstorm weather process occurred in the north of central Hunan. Among them, the heavy precipitation on June 26 had the widest range and the strongest intensity. The comprehensive analysis found that the heavy precipitation appeared in the northwest of Hunan, Dongting Lake area and central and western Hunan, causing serious flood disasters. Figure 7.1 shows the process precipitation distribution of 97

**Fig. 7.1** Precipitation distribution in Hunan Province from 08:00 June 25 to 08:00 June 28, 2012 (unit: mm)



conventional meteorological observation stations in Hunan Province. As shown in the figure, the cumulative rainfall of 19 conventional meteorological observation stations in the province is 50–100 mm, 18 stations are 100–200 mm, and 6 stations are more than 200 mm. The cumulative rainfall of Cili in Zhangjiajie and Shimen in Changde is more than 300 mm, which is 329.6 mm and 318.4 mm respectively.

Figure 7.2 shows the average circulation field from 08:00 on June 25 to 08:00 on June 28, 2012. As shown in the figure, there are two ridges and one trough inverted  $\Omega$ -shaped in the middle and high latitudes of Asia at 500 hPa, a high-pressure ridge from West Siberia to Northwest China, a wide inverted  $\Omega$ -shaped low trough near Lake Baikal, and a high-pressure ridge from East Siberia to the Sea of Japan. The subtropical high in the low latitudes of the Western Pacific is distributed in a belt, and the position is easterly. The ridge point is located near ( $130^{\circ}$  E,  $22^{\circ}$  N). The southwest monsoon is continuously strengthened during the rainstorm process. At the lower 850 hPa, the Somali cross-equatorial southwesterly airflow forms two jet centers in the range of ( $40^{\circ}$  E– $70^{\circ}$  E,  $5^{\circ}$  N– $15^{\circ}$  N) and near the Bay of Bengal, respectively. The southwesterly airflow extends to the northeast to the north of South China, which transports abundant water vapor and unstable energy for the rainstorm area. The southwest vortex in Guizhou and the stable maintenance of warm shear in the middle and lower reaches of the Yangtze River are the main causes of persistent rainstorm in Hunan.

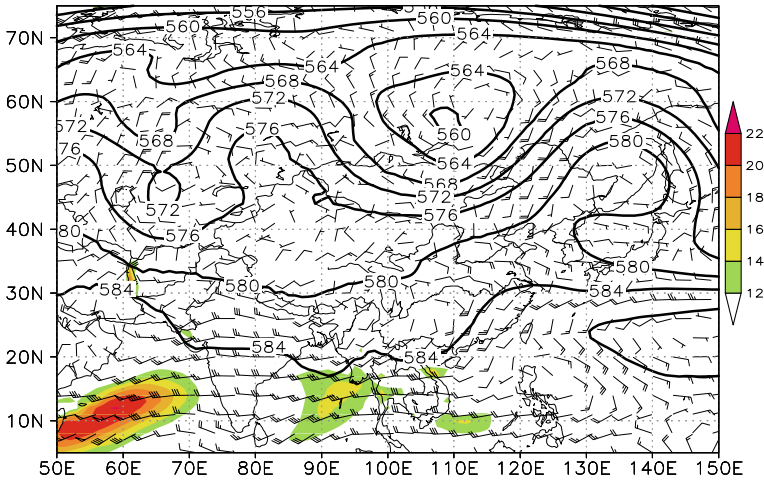


**Fig. 7.2** Average 500 hPa geopotential height field from 08:00 June 25 to 08:00 June 28, 2012 (solid line, unit: dagpm), 850 hPa wind field (wind scale, unit:  $\text{m}\cdot\text{s}^{-1}$ ) and torrent zone (shaded zone, unit:  $\text{m}\cdot\text{s}^{-1}$ )

## 7.4 Diagnostic Analysis

### 7.4.1 Non-geostrophic Wet Q Vector Horizontal Flow Field and Its Divergence Field Distribution

The 700 hPa non-geostrophic wet Q vector flow field and distribution during the peak period of this continuous rainstorm process were compared with the actual precipitation. As shown in Fig. 7.3, the non-geostrophic wet Q vector flow field is mainly characterized by divergence and convergence centers (convergence lines). The horizontal scale of these divergence and convergence centers (convergence lines) is about 200–300 km, with obvious mesoscale characteristics. At 20:00 on June 25 (figure omitted), there are two weak Q-vector convergence centers in Hunan. One is located at the junction of northeast Guizhou and northwest Hunan, and the other is located near Changsha-Zhuzhou-Xiangtan. The intensity of center  $\nabla \cdot Q^*$  is  $-12 \times 10^{-15} \text{ hPa}^{-1} \cdot \text{s}^{-3}$ , corresponding to the next 6 h respectively at the junction of northeast Guizhou and northwest Hunan, the northern part of northern Hunan and the west of central Hunan. The location of the heavy precipitation center at the junction of northeast Guizhou and northwest Hunan is basically consistent with the position of the Q vector convergence center, while the heavy precipitation center in the northern part of northern Hunan in the next 6 h is concentrated after 21 O'clock, which cannot be predicted in the Q vector divergence field at 20 O'clock, so that the phenomenon of missing forecast occurs. In addition, the strong precipitation center in Xinhua in the west of central Hunan is not consistent with the weak Q vector convergence center near Changsha-Zhuzhou-Xiangtan, and the weak Q vector convergence center of the

strong precipitation center is slightly westward. Some scholars have pointed out that (Zhang et al. 2008), the relationship between  $\omega$  and proportional is obtained when  $\omega$  is assumed to be a function with wavy characteristics, while  $\omega$  in the actual atmosphere is not a strict wavy function. Therefore, the strongest vertical motion does not necessarily correspond to the strongest Q vector convergence zone. At 02:00 on June 26 (Fig. 3a), the weak Q-vector convergence center at the junction of northeastern Guizhou and northwestern Hunan moved toward northwestern Hunan. The convergence zone covered the entire northwestern Hunan and northern northern Hunan. The center intensity was significantly enhanced, reaching  $-42 \times 10^{-15} \text{ hPa} \cdot \text{s}^{-3}$ . The Q-vector convergence center originally located near Changsha-Zhuzhou-Xiangtan weakened and tended to die out. In the next 6 h, 68 stations with precipitation greater than 50 mm and 2 stations with precipitation greater than 100 mm appeared in western Hunan, northern Huaihua, eastern Zhangjiajie and northern Changde. The heavy precipitation area was in good agreement with the strong Q-vector convergence area. At the same time, the Q vector convergence zone in northern Hunan is consistent with the falling area of heavy rainfall in the first 5 h, which makes up for the missing forecast phenomenon of heavy rainfall in northern Hunan at 20:00. At 08:00 on June 26 (Fig. 7.3b), the strong Q vector convergence zone in northwestern Hunan was further expanded, extending from southwestern Hunan to northern Hunan in a band. The original strong convergence center in northwestern Hunan was significantly weakened, and the position of the convergence center moved slightly eastward. At the same time, a weak Q vector convergence center appeared in southwestern Hunan, both centers were  $-12 \times 10^{-15} \text{ hPa}^{-1} \cdot \text{s}^{-3}$ . In addition, at the junction of the two lakes in northern Hunan, the convergence center was significantly enhanced, reaching  $-30 \times 10^{-15} \text{ hPa}^{-1} \cdot \text{s}^{-3}$ .

At 14:00 on 26 June (Fig. 3c), the Q vector convergence center in the northwest and north of Hunan merged into a convergence center, which was located at the junction of Zhangjiajie, Changde and Huaihua. The center value was  $-18 \times 10^{-15} \text{ hPa}^{-1} \cdot \text{s}^{-3}$ . The evolution of this convergence center in the first 6 h was consistent with the location of heavy precipitation in the northwest of Changde, the east of Zhangjiajie and the north of Huaihua in the first 6 h of 14:00. The weak Q vector convergence center in the southwest of Hunan disappeared, and there was no heavy precipitation weather in this area within 6 h, indicating that there was a false prediction phenomenon in the weak Q vector convergence area at 08:00. In the following 6 h, the Q vector convergence center of northwestern Hunan further moved northward, and the convergence center moved to the middle of Hubei at 20:00 (figure omitted) on 26 June, with a center value of  $-24 \times 10^{-15} \text{ hPa}^{-1} \cdot \text{s}^{-3}$ . Except for the northwest of Hunan and some areas in the north of Hunan, the other areas were divergent areas, corresponding to the weakening period of heavy precipitation in Hunan, only in the northwest of Changde and the east of Zhangjiajie. There was a small range of heavy precipitation weather, and the change trend of heavy precipitation was basically consistent with the change of Q vector convergence area in northwest Hunan. At 02:00 on 27 June (Fig. 7.3d), the position of the Q vector convergence center in the northwest of Changde did not change much, and the intensity weakened to  $-18 \times 10^{-15} \text{ hPa}^{-1} \cdot \text{s}^{-3}$ , which was consistent with the location of the continuous heavy rainfall area in the northwest of

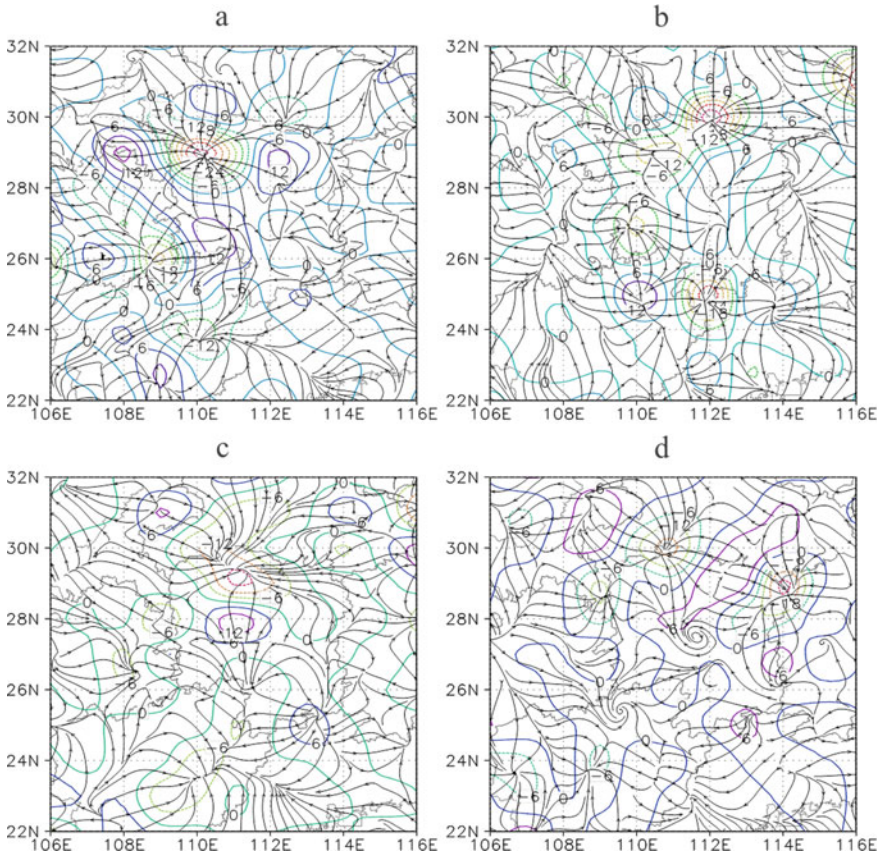


**Fig. 7.3** 700 hPa non-geostrophic wet Q vector flow field and distribution map (unit:  $10^{-15} \text{ hPa}^{-1} \cdot \text{s}^{-3}$ ) (a) 02:00 on 26 June, b) 08:00 on 26 June, c) 14:00 on 26 June, d) 02:00 on 27 June)

Change and the east of Zhangjiajie. At the same time, a convergence center with a size of  $-24 \times 10^{-15} \text{ hPa}^{-1} \cdot \text{s}^{-3}$  appeared in the east of Yueyang, corresponding to the short-term heavy rainfall weather in this area in the next 6 h. The above analysis shows that the change of non-geostrophic wet Q vector convergence zone has a good indication to the falling area of persistent heavy rainfall, and there is a good correspondence between the strong Q vector convergence zone and the heavy rainfall area, while the wet Q vector convergence center is stably maintained in a certain area, which is prone to persistent heavy rainfall.

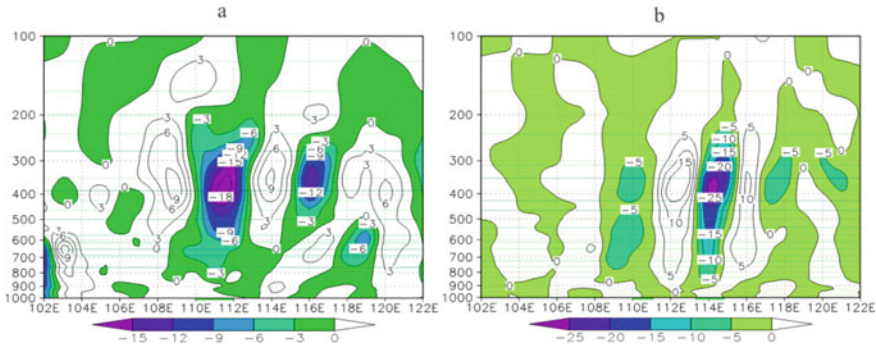


**Fig. 7.4** The meridional average ( $28^{\circ}\text{ N}$ – $30^{\circ}\text{ N}$ ) zonal vertical profile (unit:  $10^{-15}\text{ hPa}^{-1}\cdot\text{s}^{-3}$ ) (a 14:00 on 26 June, b 08:00 on 27 June)

### 7.4.2 Vertical Distribution of Non-geostrophic Wet $Q$ Vector Divergence

In order to reveal the relationship between  $\nabla \cdot Q^*$  and heavy rainfall, the heavy rainfall area ( $28^{\circ}\text{ N}$ – $30^{\circ}\text{ N}$ ) is selected as the zonal vertical profile of the meridional average  $\nabla \cdot Q^*$ . Figure 7.4 shows the vertical distribution of  $\nabla \cdot Q^*$  in the zonal direction during the peak period of heavy rainfall. As shown in Fig. 7.4, in the development stage of torrential rain, there are several “positive–negative” centers of  $\nabla \cdot Q^*$  appearing alternately near 400 hPa, and the torrential rain area corresponds to the strong negative value area of  $\nabla \cdot Q^*$ . The strongest convergence area is located in the middle troposphere between 500 and 300 hPa, and the central intensity is  $-25 \times 10^{-15}\text{ hPa}^{-1}\cdot\text{s}^{-3}$ . The negative value area corresponds to the  $\nabla \cdot Q^*$  convergence area, which will force the non-geostrophic ascending motion, namely the ascending branch of the secondary circulation. At the same time, there is a positive  $\nabla \cdot Q^*$  value area on the east and west sides of the negative value area, which corresponds to the non-geostrophic descending motion. After 08:00, 28 June (figure omitted), the middle troposphere along the east–west “positive–negative” alternating region disappeared, corresponding to the strong precipitation in Hunan weather tends to end. This indicates that the occurrence of torrential rain is not only related to the non-geostrophic ascending motion, but also related to the non-geostrophic descending motion, which is conducive to the formation of secondary circulation, and the negative value area often has a good correspondence with torrential rain.

### 7.4.3 Non-geostrophic Wet $Q$ Vector Secondary Circulation

Studies have shown that (Qiao and He 2010) there is a close relationship between the strong convective weather and the secondary circulation. The non-geostrophic



ascending and descending motions over the heavy rainfall area in Hunan are the manifestations of the secondary circulation. In order to further reveal this relationship, this paper analyzes the characteristics of the  $Q^*$  vector component and the vertical circulation in the development stage of the heavy rainfall. Figure 5a along the rainstorm area  $Q_x^*$  zonal vertical profile distribution, between  $110^\circ$  E and  $116^\circ$  E  $Q_x^*$  is “negative–positive–negative” arrangement, the rainstorm area is located in the  $Q_x^*$  negative value area on the west side of the positive and negative value of the intersection, that is, the east side of the rainstorm area  $Q_x^*$  is negative to the west, the west side of the  $Q_x^*$  is positive to the east, so there is an upward branch of the secondary circulation at the intersection of the positive and negative values on the west side of the  $Q_x^*$  negative value area, while there is a sinking branch of the secondary circulation at the intersection of the positive and negative values on the west side of the  $Q_x^*$  positive value area. In addition, the analysis of the longitudinal vertical cross section of  $Q_y^*$  along the torrential rain area (Fig. 7.5b) shows that there is also a meridional secondary circulation circle over the torrential rain area. The torrential rain area is located at the intersection of the positive and negative values on the south side of the negative  $Q_y^*$  value area, corresponding to the ascending branch of the secondary circulation, while the intersection of the positive and negative values on the south side of the positive  $Q_y^*$  value area is the descending branch of the secondary circulation. The above conclusions can be confirmed by the vertical circulation field. The  $110^\circ$  E– $111^\circ$  E,  $114^\circ$  E and  $28^\circ$  N– $29^\circ$  N near the intersection of the positive and negative values on the west side of the  $Q_x^*$ -negative area and the south side of the  $Q_y^*$ -negative area are updrafts, and the  $113^\circ$  E and  $28^\circ$  N near the intersection of the positive and negative values on the west side of the  $Q_x^*$ -positive area and the south side of the  $Q_y^*$ -positive area are downdrafts. Therefore, the secondary circulation has obvious indicative function in forecasting rainstorm and its falling area, and the analysis of non-geostrophic wet Q vector can provide a very important reference for rainstorm forecasting.

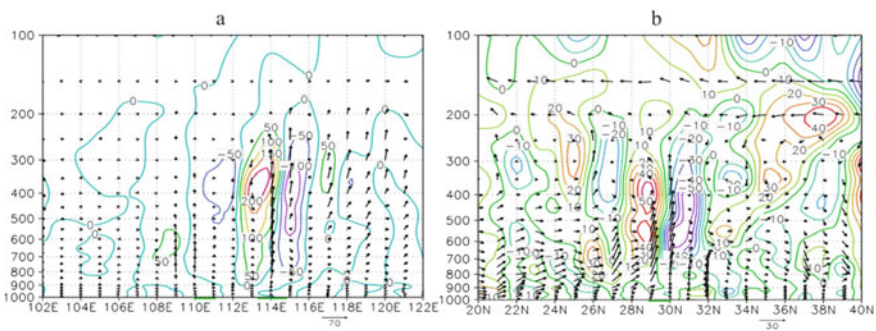


**Fig. 7.5** Meridional mean ( $28^\circ$  N– $30^\circ$  N) and latitudinal vertical profile ( $u, -50 \omega$ ) at 08:00 on 27 June (a), zonal mean ( $109^\circ$  E– $114^\circ$  E) and meridional vertical profile ( $v, -50 \omega$ ) at 08:00 on 27 June (b) (Contour, unit:  $10^{-11} \text{ m}\cdot\text{hPa}^{-1}\cdot\text{s}^{-3}$ )

## 7.5 Conclusions

In this paper, a continuous rainstorm weather process occurred in Hunan on June 25–28, 2012 is analyzed. The continuous precipitation is mainly caused by the continuous upward motion, and the strong diabatic heating is mainly caused by the strong water vapor convergence in the middle and lower layers. The relationship between non-geostrophic wet  $Q$  vector and secondary circulation and precipitation is analyzed, and the following conclusions are obtained:

- (1) The change of the non-geostrophic wet  $Q$  vector convergence zone in the middle and lower levels has a good indication to the heavy rainfall area. The strong  $Q$  vector convergence center is conducive to the occurrence of heavy rainfall, and the strong  $Q$  vector convergence center is stably maintained in a certain area, which is prone to persistent heavy rainfall.
- (2) There are multiple  $\nabla \cdot Q^*$  “positive–negative” centers appearing alternately near 400 hPa in the middle troposphere. The rainstorm area corresponds to the strong  $\nabla \cdot Q^*$  negative area, and the non-geostrophic ascending motion is forced in the  $Q^*$  convergence area. The  $\nabla \cdot Q^*$  positive area on the east and west sides of the negative area corresponds to the non-geostrophic sinking motion. The rainstorm is not only related to the non-geostrophic ascending motion, but also the non-geostrophic sinking motion.
- (3) The  $W$  vector component can well reveal the spatial distribution characteristics of the secondary circulation. During the peak period of the torrential rain,  $X$  and  $Y$  are alternately arranged in multiple “positive–negative” centers along the latitudinal and longitudinal directions, respectively. The torrential rain area is often located near the ascending branch of the secondary circulation at the intersection of the positive and negative values on the west side of the  $X$  negative area and the south side of the  $Y$  negative area.

**Acknowledgements** The paper is funded by the following project: China Meteorological Administration Forecaster Special Project (CMAYBY2020-085); Key Projects of Hunan Meteorological Bureau (XQKJ22A004); Key Fields Research and Development Project of Hunan Provincial Department of Science and Technology (2019SK2161); Hunan Business Capacity Building (NLJS14); Key Projects of Hunan Meteorological Bureau (XQKJ19B016).

## References

- Chen HZ, Zhang DS, Luo ZR (2009) Diagnostic analysis of heavy rainfall in north Hunan Province. *Torrential Rain Disasters* 28(4):373–376
- Gao LX, Liu C, Yang XX et al (2018) Ageostrophic wet  $Q$ -vector analysis of a persistent torrential rainfall event in the northwest of Shandong Province. *J Mar Meteorol* 38(3):75–82
- Gao S, Xiao TG, Wu LJ (2019) Diagnostic analysis of wet  $Q$ -vector for a rainstorm process in the middle and lower reaches of Yangtze River. *Meteorol Environ Sci* 42(3):58–67

- Hoskins BJ, Draghici I, Davies HC (1978) A new look at the  $\omega$ -equation. *Quart J Roy Meteor Soc* 104(11):31–38
- Li SS, Li GP (2017) Diagnostic analysis based on wet Q-vector of a shear line with rain on the east side of Qinghai-Tibetan Plateau under the saddle pattern circulation background field. *Plateau Meteorol* 36(2):317–329
- Li Y, Zhang TF, Guo FR (2002) Ageostrophic wet Q-vector analysis of a persistent rainstorm process in Yunnan. *J Nanjing Inst Meteorol* 25(2):259–264
- Liu YC (2006) Wet Q-vector analysis of a continued heavy rain process over the eastern Qinghai-Xizang plateau. *Meteor Mon* 32(12):43–49
- Qiao CG, He Z (2010) Ageostrophic wet Q-vector analysis of a rainstorm process in Henan. *Meteorol Environ Sci* 33(2):48–52
- Ran LK, Li Z, Zhang YB et al (2019) The diagnostic analysis of Q vector during a heavy rain event in north China. *Torrential Rain Disasters* 38(1):17–30
- Shi WZ, Zhang PP, Wu T et al (2008) Contrastive analysis of heavy rain cases in Hubei province. *Torrential Rain Disasters* 27(3):219–224
- Song QZ, Qiao CG, Gao YY (2009) Synoptic analysis of the super rainstorm process in Henan. *Meteorol Environ Sci* 32(3):6–9
- Yang XY, Cao XX (1995) An analysis of the relationship between quasi-geostrophic Q-vector and heavy rain. *Meteor Mon* 21(11):17–21
- Yi Y, Duan X, Pan L (1999) A quasi-geostrophic Q-vector analysis of Kunming quasi-stationary front. *Meteor Mon* 25(8):6–10
- Zhang XW (1998) An expression of the wet Q-vector and application. *Meteor Mon* 24(8):3–7
- Zhang X (1999) The expression of the modified Q-vector and its application. *J Trop Meteorol* 15(2):162–167
- Zhang GZ, Li G, Bai JH et al (2008) Role of coupled jets at different levels in Henan regional heavy rain during 12–14 July 2007. *Meteorol Environ Sci* 31(2):7–12